Exact Analytical and Numerical Solutions for Convective Heat Transfer in a Semi-Spherical Extended Surface with Regular Singular Points

Nematollahzadeh, Ali*, +; Jangara, Hossein

Chemical Engineering Department, University of Mohaghegh Ardabili, P.O. Box 179, Ardabil, I.R. IRAN

ABSTRACT: *In this study, an exact analytical solution for the convective heat transfer equation from a semi-spherical fin was presented. To obtain a mathematical model, the system was assumed to be a lump in the vertical direction and the governing equation in the Cartesian coordinate was transferred to the Mathieu equation. The exact solution was compared with numerical results such as the finite difference method and midpoint method with Richardson extrapolation (Midrich). Not surprisingly, the exact solution prevailed over the numerical solutions in terms of accuracy and ease of use. Furthermore, the effect of Biot number on the heat transfer of the fin and the fine performance was investigated. The relative error of the results obtained from the analytical and numerical solutions at the base, center, and tip of the fin was 0, 7.72, and 40.25 percent, respectively. The results showed that the relative error between the analytical and numerical solutions depends on the Biot number and varies as a function of the fin length. The obtained analytical solution could be encouraging from different mathematical and industrial applications' points of view.*

KEYWORDS: *Convective heat transfer; Semi-spherical extended surface; Exact analytical solution; Mathieu's equation.*

INTRODUCTION

Extended surfaces or fins are employed to enhance the rate of heat transfer to or from the surrounding medium [1]. Indeed, the fins are employed for the removal of waste heat or enhance the heat transfer to another medium or to the environment, especially by convection heat transfer. Convective heat transfer utilizes the forced or free motion of a fluid.

Thus far, several types of fins such as triangular, rectangular, circular, and spherical fins are used in many industrial applications such as chemical processing equipment, aerospace, and electronic components. For instance, pin fins and fined tubes are commonly used in electronic devices, power transformers, and petroleum industries, especially due to their high surface area, ease of construction and mathematical modeling. However, as the rate of convective heat transfer depends on the temperature gradient, the surface area of the fin, and the heat transfer coefficient, there is a growing demand for an optimal design of fins. Therefore, with the aim of the search for the best performing extended surface, the thermal analysis

** To whom correspondence should be addressed.*

+ E-mail: nematollahzadeha@uma.ac.ir

1021-9986/2021/3/980-989 10/$/6.00

of plate, semi-circular and Rhombus shape pin fins was analyzed by different researchers [2-5]. In line with previous studies on fins with non-uniform cross-section, semi-spherical fins (Fig. 1) are also considered by several authors [6-8]. Nevertheless, most previous studies on heat transfer in fins with complex geometry give only numerical or approximate solutions for the governing equations. While, exact analytical solutions are definitely more accurate and valuable than numerical or approximate solutions [9]. Nonetheless, in most cases, it is very difficult or even impossible to obtain an exact analytical solution for differential equations of conductive heat transfer fins, especially for a non-linear or noncanonical form of the differential equations. Even with one nonlinear term, the equation is not amenable to an exact analytical solution. Consequently, most previous studies have been based on numerical techniques or approximate methods such as perturbation homotopy method [10] for more realistic problems. Since the exact analytical solutions are reliable, they will be useful for validating numerical and experimental results. Furthermore, for any changes in the input parameters of a given equation, the numerical procedure has to be repeated. This can be quite a time consuming especially when there is a need for high accuracy by increasing the step size of the calculations.

Moitsheki [11] studied different types of radial fins and provided exact solutions to observe the thermal performance of the fins. *Unal* [12] used an analytical solution to obtain temperature distribution of straight rectangular fin with temperature-dependent internal heat generation and heat transfer coefficient. *Ganji* and *Dogonchi* [13] conducted an analytical investigation on heat convective transfer in longitudinal fin with temperature-dependent thermal conductivity and heat source. They obtained temperature distribution in the fin by using the Differential Transformation Method (DTM). In another study, DTM was used for predicting the performance of convective straight fins with temperature-dependent thermal conductivity by *Joneidi et al.* [14]. *Rahimi Petroudi et al.* [15] employed the homotopy perturbation method (HPM) for the convective rectangular porous fin to obtain an approximate solution. *Jing Ma et al.* [16] considered a rectangular porous fin with a temperature-dependent convective heat transfer coefficient. They used the Spectral Collocation Method (SCM) and compared their results with HPM and Finite Volume Method (FVM) to verify the results. *Ganji et al.* [17] determined temperature distribution for annular fins with temperature-dependent thermal conductivity by using HPM. *Turkyilmazoglu* [18] conducted an exact solution to heat transfer in straight fins of varying exponential shape with temperature-dependent thermal conductivity and convection heat transfer coefficient. *Atouei et al.* to predict the temperature distribution in convective-radiative semi-spherical fins with temperature-dependent properties used collocation method and compared their results with the Least Square Method (LSM) and numerical solution [6]. Recently *Patel* and *Meher* [19, 20], proposed ADSTM which is a combination of the Adomian Decomposition Method and Sumudu transform method. They obtained temperature distribution and fin efficiency for a convective longitudinal fin with internal heat generation and porous fin with different fractional-order values. Also, *Patel* and *Meher* [21, 22] investigated the temperature distribution in the rectangular porous fin and convective-radial fin with temperature-dependent thermal conductivity. They applied ADSTM to obtain thermal performance and ultimately compared their results with numerical solution outcomes.

Hatami et al. [7] studied fully wet semi-spherical porous fins and also investigated the effects of porosity, Rayleigh, and Lewis number on the performance of the fin. *Sabbaghi et al.* [8] considered a semi-spherical fin with simultaneous heat and mass transfer and used an analytical method to observe the efficiency of the fin.

The present paper provides an exact analytical solution for the governing differential equation of a semi-spherical fin. For this purpose, after a variable change on the differential equation, the exact solution has been obtained. Also, the governing differential equation was solved by two different numerical methods, namely Richardson extrapolation and finite difference methods. Finally, the exact analytical solution was compared with the numerical solution.

PROBLEM DESCRIPTION AND GOVERNING EQUATIONS

As shown in Fig. 1, a semi-spherical fin with radius R was considered lump in polar directions (zenith and inclination angle) and it was assumed that the heat conduction occurs in the other direction. The fin was assumed to be isotropic type and therefore the thermal conductivity k was assumed to be constant.

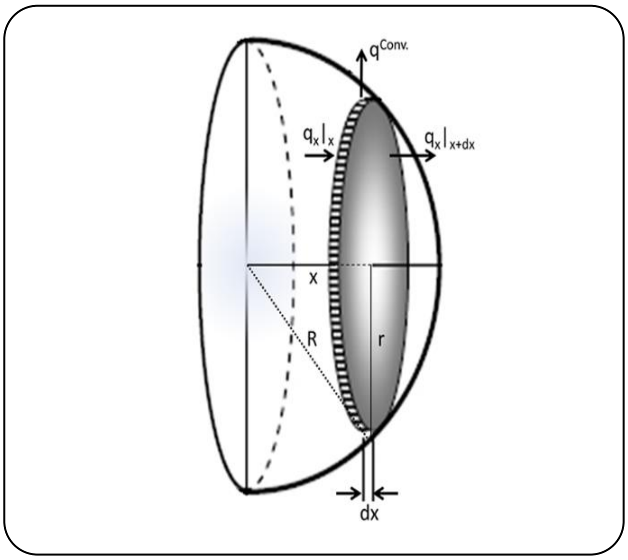

Fig. 1: Schematic representation of conduction and convection heat transfer in a semi-spherical fin.

Using Fourier's law of conduction, the energy balance at the steady-state condition can be written as follows [6]:

$$-kA(x)\left.\frac{dT}{dx}\right|_x + kA(x)\left.\frac{dT}{dx}\right|_{x+dx} - hP(x)\,dx\,(T - T_\infty) = 0 \tag{1}$$

where, *A(x)* and *P(x)* are the differential element area and pyramid, respectively:

$$A(x) = \pi\left(R^2 - x^2\right) \tag{2a}$$

$$P(x) = 2\pi\sqrt{R^2 - x^2} \tag{2b}$$

Taylor expansion of the second term of Eq. 1 gives:

$$kA(x)\left.\frac{dT}{dx}\right|_{x+dx} = kA(x)\left.\frac{dT}{dx}\right|_x + \left.\frac{d}{dx}\left(kA(x)\frac{dT}{dx}\right)\right|_x dx + \ldots \tag{3}$$

Omitting the higher terms than the second term in Eq. 3 and inserting in Eq. 1, gives the following governing equation:

$$\left(R^2 - x^2\right)\frac{d^2T}{dx^2} - 2x\frac{dT}{dx} - \frac{2h}{k}\sqrt{R^2 - x^2}\,(T - T_\infty) = 0 \tag{4}$$

The following boundary conditions can be considered:

Case i) Insulated tip:

B.C.1) $T(x = 0) = T_b$ (4a-i)

B.C.2) $\left.\dfrac{dT}{dx}\right|_{x=R} = 0$ (4b-i)

Case ii) Constant temperature at the tip:

B.C.1) $T(x = 0) = T_b$ (4a-ii)

B.C.2) $T(x = R) = \text{finite}$ (4b-ii)

Eq. 4 was non-dimensionalized using the following dimensionless parameters:

$$\theta = \frac{T - T_\infty}{T_b - T_\infty}\ ,\quad \xi = \frac{x}{R}\ ,\quad Bi = \frac{hR}{3k} \tag{5}$$

$$\left(1 - \xi^2\right)\frac{d^2\theta}{d\xi^2} - 2\xi\frac{d\theta}{d\xi} - 6Bi\sqrt{1 - \xi^2}\,\theta = 0 \tag{6}$$

It follows that *ξ=±1,* □ are regular singular points and all other finite values of *ξ* are ordinary points of Eq. (6). The non-dimensionless boundary conditions are as follow:

$$\theta(\xi = 0) = 1\ ,\ \theta(\xi = 1) = \text{finite} \tag{7}$$

To resolve the singular point issue, the second boundary condition can be written as follows:

$$\left.\frac{d\theta}{d\zeta}\right|_{\zeta=1} = 0 \tag{8}$$

This means that the tip of the fin is assumed to be insulated as previously used by many authors [23-25].

ANALYTICAL SOLUTION

Exact analytical solution

Different exponential and triangular transformation functions were tried to obtain an ODE with possible analytical solutions. The following variables heuristically were chosen to simplify the governing equation (Eq.(6)):

$$\xi = \sin(\varphi)\ ,\ \theta = \frac{Y}{\cos(\varphi)} \tag{9}$$

By substitution of the aforementioned variables in Eq. (6), the differential governing equation and the boundary conditions becomes as follows:

$$\frac{d^2Y}{d\varphi^2} + [1 - 6Bi\cos(\varphi)]\,Y = 0 \tag{10}$$

$$Y(\varphi = 0) = 1 \tag{10a}$$

$$\left.\frac{dY}{d\varphi}\right|_{\varphi=\frac{\pi}{2}} = -\theta(1) \tag{10b}$$

The general periodic solution to Eq. (10) can be found by using Taylor expansion for cos (φ) and substituting the following trial solution:

$$Y = \sum_{n=0}^{\infty}\left(A_n \cos(n\varphi) + B_n \sin(n\varphi)\right) \tag{11}$$

or

$$Y = \sum_{n=0}^{\infty} A_n \phi^{n+r} \tag{12}$$

By substituting Eq. 12 into Eq. 10 and making the coefficient of each function identically equal to zero, the following recursion relation was found for A_{2k} and A_{2k+1}:

$$Y = C_1 \sum_{k=0}^{\infty} A_{2k}\varphi^{2k} + C_2 \sum_{k=0}^{\infty} A_{2k+1}\varphi^{2k+1} \tag{13}$$

where

$$\begin{aligned} A_0 &= 1 \\ A_1 &= 12Bi - 2 \\ A_2 &= \frac{2}{3} - 12Bi + 24Bi^2 \\ A_3 &= -\frac{4}{45} + \frac{88}{15}Bi - 32Bi^2 + \frac{32}{5}Bi^3 \\ &\vdots \end{aligned}$$

$$\sum_{k=0}^{\infty} A_{2k}\phi^{2k} \equiv \sum_{k=0}^{\infty} A_m^n \cos(m\phi/2) = M_C(4, 12Bi, \frac{1}{2}\phi)$$

$$\sum_{k=0}^{\infty} A_{2k+1}\phi^{2k+1} \equiv \sum_{k=0}^{\infty} A_m^n \sin(m\phi/2) = M_S(4, 12Bi, \frac{1}{2}\phi)$$

Where, m and n are odd or even numbers and M_C and M_S are Mathieu functions [26, 27]. Therefore, the analytical solution for the governing equation (Eq. (6)) is as follows:

$$Y(\phi) = C_1 M_C(4, 12Bi, \frac{1}{2}\phi) + C_2 M_S(4, 12Bi, \frac{1}{2}\phi) \tag{14}$$

or

$$\theta(\xi) = \frac{M_C\left(4, 12Bi, \frac{1}{2}\sin^{-1}(\xi)\right)}{\sqrt{1-\xi^2}} - \frac{\left(2\theta(1) + M'_C\left(4, 12Bi, \frac{\pi}{4}\right)\right) M_S\left(4, 12Bi, \frac{1}{2}\sin^{-1}(\xi)\right)}{M'_S\left(4, 12Bi, \frac{\pi}{4}\right)\sqrt{1-\xi^2}} \tag{15}$$

Where, M'_C and M'_S are the *MathieuPrime* or the derivatives of *Mathieu* functions. To obtain *θ(1)*, t he second boundary condition (i.e. $\left.\frac{d\theta}{d\zeta}\right|_{\zeta=1} = 0$) can be applied.

$$\theta(1) = \frac{M_C\left(4, 12Bi, \frac{\pi}{4}\right) M'_S\left(4, 12Bi, \frac{\pi}{4}\right)}{2M_S\left(4, 12Bi, \frac{\pi}{4}\right)} - \frac{1}{2}M'_C\left(4, 12Bi, \frac{\pi}{4}\right) \tag{16}$$

Therefore, the following single solution can be obtained:

$$\theta(\xi) = \frac{M_C\left(4, 12Bi, \frac{1}{2}\sin^{-1}(\xi)\right)}{\sqrt{1-\xi^2}} - \frac{M_C\left(4, 12Bi, \frac{\pi}{4}\right)}{M_S\left(4, 12Bi, \frac{\pi}{4}\right)} \frac{M_S\left(4, 12Bi, \frac{1}{2}\sin^{-1}(\xi)\right)}{\sqrt{1-\xi^2}} \tag{17}$$

Although the value of *θ(1)* can be achieved from Eq. 16, it was solved for different values of *Bi* number and the following simple relationship was obtained by curve fitting:

$$\theta(1) = \frac{(1 + mBi)^p}{(1 + nBi)^q} \tag{18}$$

where m=0.051315, n=1.254745, p=-9.32588, and q=1.207541, and the regression coefficient (R^2) is 0.9999998.

The transferred heat from the base of the fin can be calculated from the following formula:

$$q = -kA\left.\frac{dT}{dx}\right|_{x=0} \tag{19}$$

or in the dimensionless form:

$$Q = \left.\frac{d\theta(\xi)}{d\xi}\right|_{\xi=0} = \frac{1}{2}\frac{M_C\left(4,12Bi,\frac{1}{4}\pi\right)}{M_S\left(4,12Bi,\frac{1}{4}\pi\right)} \tag{20}$$

The fin performance can be calculated as follows:

$$\eta = \frac{q}{hA_f(T_b - T_\infty)} = \frac{1}{8Bi}\frac{M_C\left(4,12Bi,\frac{1}{4}\pi\right)}{M_S\left(4,12Bi,\frac{1}{4}\pi\right)} \tag{21}$$

where A_f is the fin surface area and $\lim_{Bi\to 0}\{\eta\} = 1$.

Numerical analyses

To compare the exact analytical solution with the numerical solution, the finite difference method (h=0.0001) and Richardson extrapolation (*Midrich*) [28] were employed. Midrich method is a midpoint method that is used for solving linear boundary value problems (BVPs) and it can handle end-point singularities [29, 30]. For Midrich method the following formulas were used:

$$\theta = \theta(h) + kh^p + O\left(h^{p+1}\right) \tag{22}$$

$$\theta(\xi)_{Num.} = \frac{2^p\theta\left(\frac{h}{2}\right) - \theta(h)}{2^p - 1} \tag{23}$$

where $\theta(h)$ and $\theta(h/2)$ are the approximate value for $\theta(\xi)$ given by the finite difference method with step sizes of h and $h/2$, and p=2. Also, the governing differential equation was discretized by the finite difference method and the nonlinear equations system was solved by Newton's method.

RESULTS AND DISCUSSION

Exact Analytical solution

The heat transfer governing equation (Eq. 6) is a boundary value problem (BVP) with three finite regular singular points at -1, 1, and ∞. On the other hand, the point at ξ =1 belongs to the boundary condition as well. However, as the boundary condition at the regular singular point (ξ =1) is specified by the normal derivative of the function on a surface, the constants of the answer were determined with no problem. It is worth mentioning that the solution was obtained by power series (i.e. *Mathieu*) around zero, therefore, it is anticipated to be more accurate near zero with fewer terms of the series.

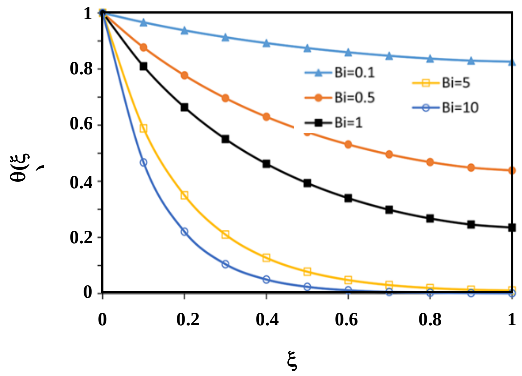

Fig. 2: Effect of Bi number on temperature distribution in the fin obtained from the analytical solution.

The constant *Bi* in Eq. 6 and the solution represents the Biot number, the ratio of the heat transfer resistance inside of a body to the heat transfer resistance between the surroundings and the surface of the body. The *Bi* number is defined as the following:

$$Bi = \frac{hL_c}{k} \tag{24}$$

Where L_c is the characteristic length of the object of study and defined as the volume of the body divided by the surface area of the body. For a spherical body L_c= R/3.

Temperature distribution at different *Bi* numbers was obtained from the exact analytical solution and presented in Fig. 2. Obviously, by increasing the *Bi* number the rate of heat transfer increases, which is in good agreement with the results reported by *Atouei et al* [6].

As can be seen in Fig. 2, a small *Bi* number leads to very low-temperature gradients or a uniform temperature distribution throughout the fin, implying low resistance to transmission by conduction. Therefore, at small values for *Bi* numbers, the fin can be assumed to be a lumped system. However, at large *Bi* numbers, the temperature gradient is considerable.

Numerical solutions

Richardson extrapolation

To solve the ODE numerically, different approaches were carefully chosen. In between, midpoint method

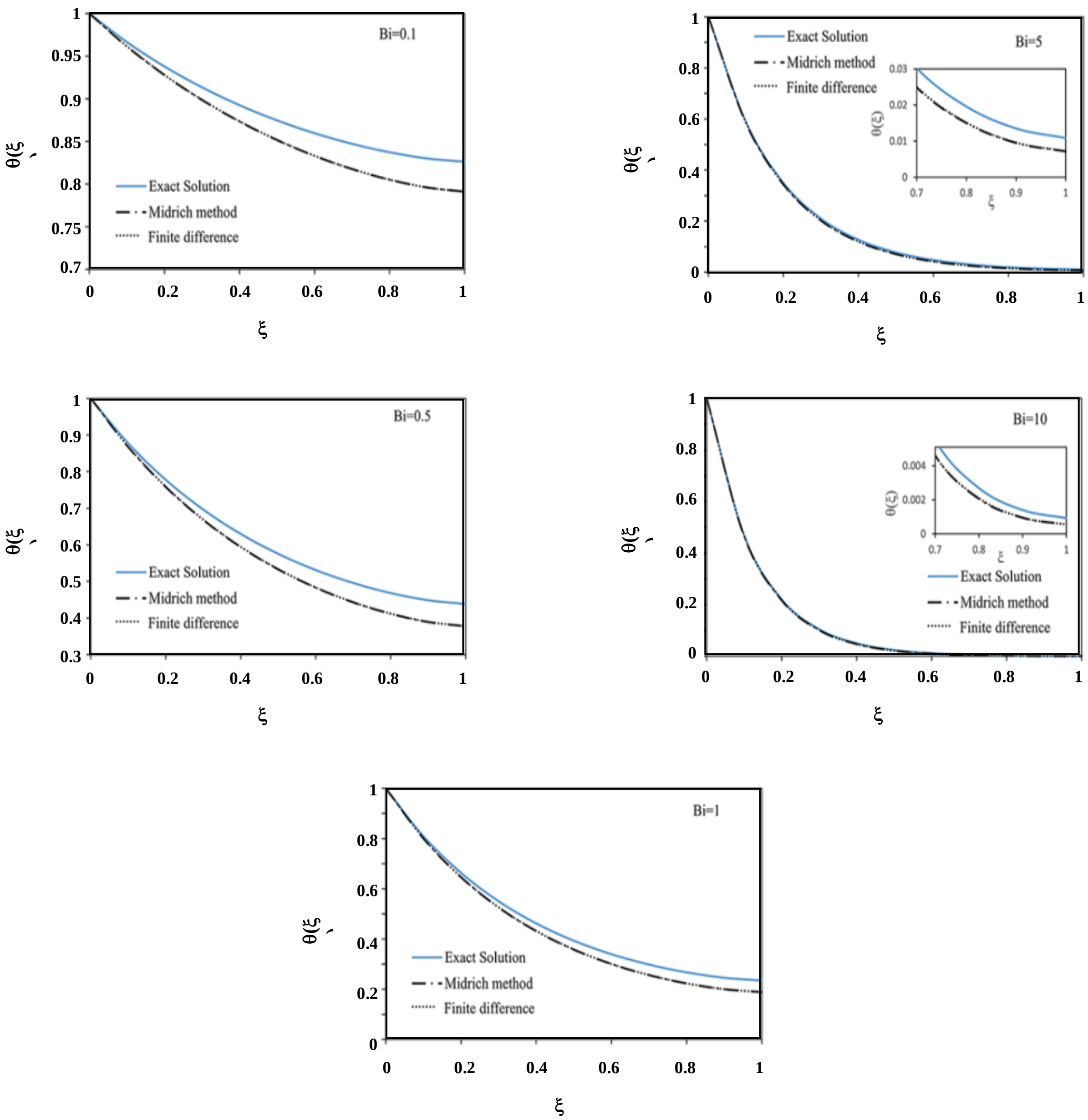

Fig. 2: ***Effect of Bi number on temperature distribution in the fin obtained from the analytical solution.***

with Richardson extrapolation (Midrich) and finite difference method could be employed successfully. Midrich method can work for ODEs with end-point singularities [31, 32]. Fig. 3 shows the temperature distribution obtained by Richardson extrapolation and finite difference methods. Results revealed that these solutions follow the same trend as the exact analytical solution.

As can be seen in Fig. 3, at small values of *Bi* the difference between the analytical and numerical methods is remarkable, while at large *Bi* values it the error levels off. in the ODE the absolute error is a function of the last term coefficient of the ODE (here the *Bi* number). Since the ODE is singular at the right endpoint, it was impossible to use the trapezoidal method when the coefficient of the last term in the differential equation (*i.e. Bi*) was too small. However, the midpoint method could be useful at a bit high value of the last term coefficient. Anyhow, to achieve a numerical solution for the BVP, the absolute error was increased, this inserts a huge error in the solution.

Table 1: Comparison of the exact analytical solution with numerical analysis for Bi=10.

ξ	Exact Solution ($\theta(\xi)_{Exa.}$)	Richardson Extrapolation ($\theta(\xi)_{Num.}$)	ΔE_R	Finite difference method ($\theta(\xi)_{Num.}$)	ΔE_R
0	1.000	1.000	0.00	1	0.00
0.1	0.46732	0.46463	0.58	0.4682	0.19
0.2	0.22042	0.21677	1.66	0.2184	0.92
0.3	0.10464	0.1012	3.29	0.102	2.52
0.4	0.04989	0.04713	5.53	0.0475	4.79
0.5	0.02384	0.02178	8.64	0.022	7.72
0.6	0.01142	0.01004	12.08	0.0101	11.56
0.7	0.0055	0.00461	16.18	0.0046	16.36
0.8	0.00269	0.00206	23.42	0.0021	21.93
0.9	0.0014	0.00095	32.14	0.000956	31.71
1.0^-	0.00092	0.00055	39.37	0.00055	40.25

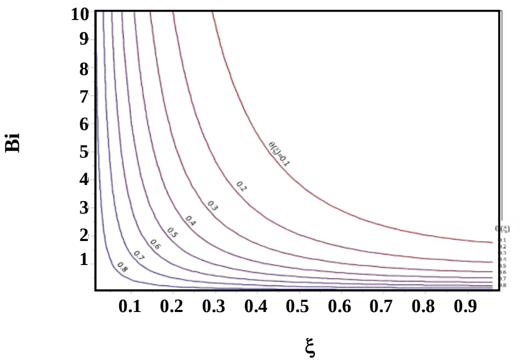

Fig. 4: Temperature distribution contour Bi-ξ plot for semi-spherical fin at dimensionless temperatures.

Temperature distribution in the fin at different *Bi* numbers is shown in Fig. 4. The results showed that at high *Bi* numbers there is a large temperature gradient between the base (ξ =0) and tip (ξ=1) of the fin and the rate of heat transfer is higher in comparison with relatively small *Bi* numbers. It means that for small *Bi* numbers, the temperature gradient is small and when *Bi=0* the temperature gradient approaches zero or there is no temperature difference between the base and tip of the fin.

Comparison of the exact solution with the numerical solutions

To validate the exact analytical solution of the differential equation the results were compared with the Richardson extrapolation and finite difference method results. Also, the relative error was calculated through the following formula and presented in Table 1.

$$\Delta E_R(\xi) = \frac{\left|\theta(\xi)_{Exa.} - \theta(\xi)_{Num.}\right|}{\theta(\xi)_{Exa.}} \times 100 \quad (25)$$

The results show that the employed numerical methods result in a larger error in comparison with the exact analytical method.

As can be seen in Table 1, the relative error between the exact analytical solution and different numerical methods are quite similar. As mentioned before, this similarity happens at large values of Bi number. However, the error increases by increasing ξ and reaching the tip of the fin (Fig. 5). The increase in the error is anticipated as ξ=1 is a regular singular point. Therefore, the answer was determined at a close neighbor to the tip of the fin at ξ= 0.99999999999. Also in Fig. 5 error residuals (i.e. $|\theta_{Exa.}- \theta_{Num.}|$) are plotted at different *Bi* numbers. Along the fin length the error residuals increase. However, there is not an especial trend between the error residuals and order of *Bi* numbers.

To better elucidate the error between the analytical and numerical methods, the relative error percentages at the tip of the fin (at ξ=1), where the error is the highest, were plotted versus *Bi* number (Fig. 6). A decay equation (Eq. (21)) was well fitted to the data with a high regression coefficient of R^2=0.9998. As can be seen in Fig. 6 the relative errors increase exponentially at least up to *Bi*=10.

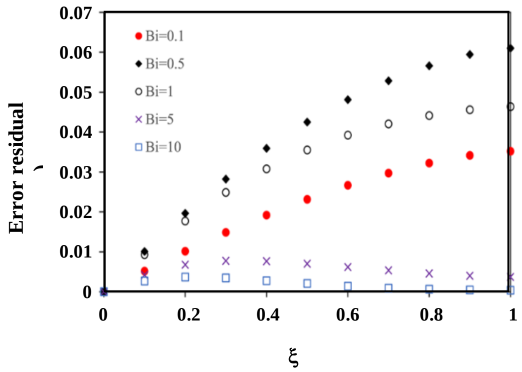

Fig. 5: Error residuals along the fin at different Bi numbers.

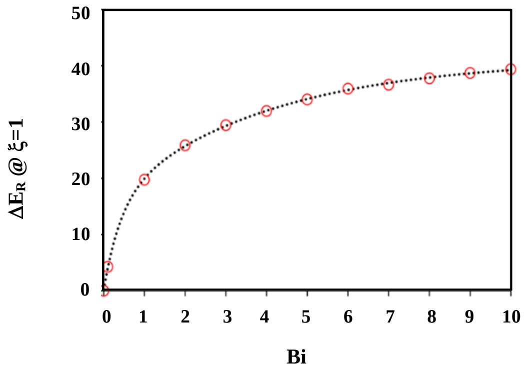

Fig. 6: Relative error at the tip of the fin versus Bi number. The dashed line shows the fitted curve.

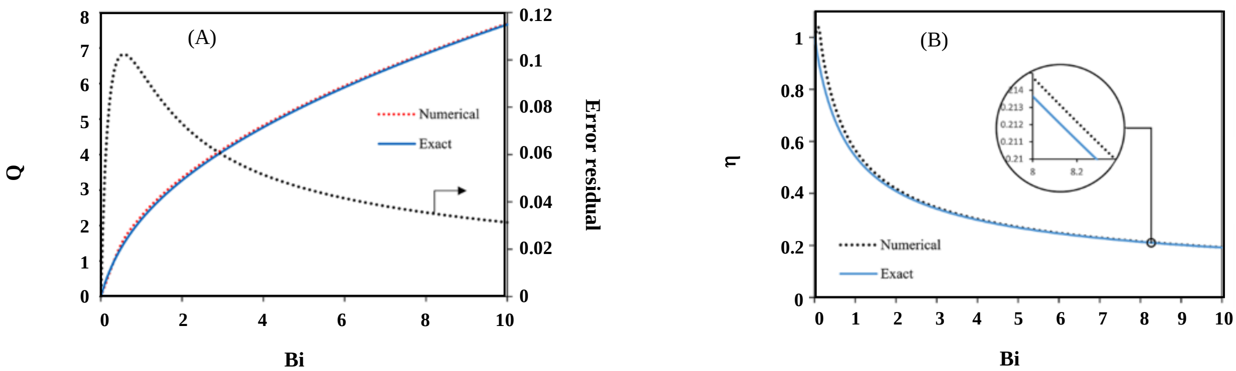

Fig. 7: Transferred heat from the fin and the error residual between the analytical and numerical method (central difference with h=10^{-5}) (A), and the fin performance (B).

$$\Delta E_R \big|_{\xi=1} = 41.19876 - 25.62100 e^{-0.25607 Bi} - 15.43460 e^{-2.37614 Bi}, \quad R^2 = 0.9998 \tag{25}$$

The transferred heat from the fin and the fin performance was calculated through the analytical Eqs. (20) and (21), and using central finite difference with 4th order accuracy with a uniform grid spacing of 10^{-5}. The results are plotted versus *Bi* and shown in Fig. 7. As can be seen in Fig. 7, the error residuals increase rapidly then decrease to lower values.

In this study, convective heat transfer in a semi-spherical fin was investigated. Hence, the linear differential equation of energy balance with singularities at the end-point on the semi-spherical fin was considered and an exact analytical solution was successfully obtained to analyze the temperature distribution along the fin. To verify the solution, Richardson extrapolation which is a midpoint method appropriate for end-point singular boundary value problems, and also finite difference method were employed. It was shown that the relative error between the analytical and numerical solutions depends on the *Biot* number. Furthermore, for the temperature distribution, the results revealed that the error is small close to the base of the fine and exponentially increases approaching the tip of the fin. While, the transferred heat and fin performance results showed that there is a large error close to the base of the fin. Since generally, an exact analytical solution is more accurate, reliable, and easy to use, the solution can be quite encouraging from different applications and mathematical points of view.

Nomenclature

A	Differential element area (m^2)
Bi	Biot number

h	Heat transfer coefficient (W/ m^2K)
k	Thermal conductivity (W/ mK)
m, n, p, q	Constants
M_C, M_S	Mathieu functions
P	Differential element pyramid (m)
q	Heat transfer flux (W/m)
Q	Dimensionless heat transfer flux
R	Fin radius (m)
r	Radius (m)
T	Temperature (ºC)
Tb	Fin base temperature (ºC)
T_{inf}	Ambient temperature (ºC)
θ	Dimensionless temperature
x	Fin direction
Y	Transformation function
ξ	Dimensionless distance
ϕ	Angle
η	Fin performance

Received : Aug. 13, 2019 ; Accepted : Jan. 27, 2020

REFERENCES

[1] Kraus, A.D., Aziz A., Welty J., "Extended Surface Heat Transfer", John Wiley & Sons Inc. (2002).

[2] Yadav, S., Verma K.A., Ray M., Pandey K.M., Thermal Analysis of Semi-Circular Pin Fins for Application in Electronics Cooling, *International Journal of Recent Technology and Engineering*, **8(2)**: 2366-2374 (2019).

[3] Subahan K., Siva Reddy E., Meenakshi Reddy R., CFD Analysis of Pin-Fin Heat Sink Used in Electronic Devices, *International Journal of Scientific and Technology Research*, **8(9)**: 562-569 (2019).

[4] Saha S.K., Emani M.S., Ranjan H., Bharti A.K., Heat Transfer Enhancement in Plate and Fin Extended Surfaces, in *SpringerBriefs in Applied Sciences and Technology*, 1-145 (2020).

[5] Belinskiy B.P., Hiestand J.W., Weerasena L., Optimal Design of a Fin in Steady-State, *Applied Mathematical Modelling*, **77**: 1188-1200 (2020).

[6] Atouei S., Hosseinzadeh K., Hatami M., Ghasemi S.E., Sahebi S., Ganji D., Heat Transfer Study on Convective–Radiative Semi-Spherical Fins with Temperature-Dependent Properties and Heat Generation Using Efficient Computational Methods, *Applied Thermal Engineering*, **89**: 299-305 (2015).

[7] Hatami M., Ahangar G.R.M., Ganji D., Boubaker K., Refrigeration Efficiency Analysis for Fully Wet Semi-Spherical Porous Fins, *Energy Conversion and Management*, **84**: 533-540 (2014).

[8] Sabbaghi, S., Rezaii A., Shahri G.R., Baktash M., Mathematical Analysis for the Efficiency of a Semi-Spherical Fin with Simultaneous Heat and Mass Transfer, *International Journal of Refrigeration*, **34(8)**: 1877-1882 (2011).

[9] Hayat T., Ashraf M.B., Shehzad S.A., Alsaedi A.. *Mixed Convection Flow of Casson Nanofluid over a Stretching Sheet with Convectively Heated Chemical Reaction and Heat Source/Sink*, (2015).

[10] Bilal Ashraf, M., Hayat T., Alsaedi A., Shehzad S.A., Soret and Dufour Effects on the Mixed Convection Flow of an Oldroyd-B Fluid with Convective Boundary Conditions, *Results in Physics*, **6**: 917-924 (2016).

[11] Moitsheki R., Steady Heat Transfer Through a Radial Fin with Rectangular and Hyperbolic Profiles, *Nonlinear Analysis: Real World Applications*, **12(2)**: 867-874 (2011).

[12] Ünal H., Temperature Distributions in Fins with Uniform and Non-Uniform Heat Generation and Non-Uniform Heat Transfer Coefficient, *Int. J. Heat Mass Transfer*, **30(7)**: 1465-1477 (1987).

[13] Ganji D., Dogonchi A., Analytical Investigation of Convective Heat Transfer of a Longitudinal Fin With Temperature-Dependent Thermal Conductivity, Heat Transfer Coefficient and Heat Generation, *International Journal of Physical Sciences*, **9(21)**: 466-474 (2014).

[14] Joneidi A., Ganji D., Babaelahi M., Differential Transformation Method to Determine Fin Efficiency of Convective Straight Fins with Temperature-Dependent Thermal Conductivity, *International Communications in Heat and Mass Transfer*, **36(7)**: 757-762 (2009).

[15] Petroudi R.I., Ganji D.D., Shotorban B.A., Nejad K.M., Rahimi E., Rohollahtabar R., Taherinia F., Semi-Analytical Method for Solving Non-Linear Equation Arising Of Natural Convection Porous Fin, *Thermal Science*, **16(5)**: 1303-1308, (2012).

[16] Ma J., Sun Y., Li B., Chen H., Spectral Collocation Method for Radiative–Conductive Porous Fin with Temperature-Dependent Properties, *Energy Conversion and Management*, **111**: 279-288 (2016).

[17] Ganji D.D., Ganji Z.Z., Ganji D.H., Determination of Temperature Distribution for Annular Fins with Temperature Dependent Thermal Conductivity by HPM, *Thermal Science*, **15**: 111-115, (2011).

[18] Turkyilmazoglu M., Exact Solutions to Heat Transfer In Straight Fins of Varying Exponential Shape Having Temperature Dependent Properties, *International Journal of Thermal Sciences*, **55**: 69-75 (2012).

[19] Patel T., Meher R., Adomian Decomposition Sumudu Transform Method for Solving a Solid and Porous Fin with Temperature Dependent Internal Heat Generation, *Springer Plus*, **5(1)**: 489- (2016).

[20] Patel T., Meher R., Adomian Decomposition Sumudu Transform Method For Convective Fin with Temperature-Dependent Internal Heat Generation and Thermal Conductivity of Fractional Order Energy Balance Equation, *International Journal of Applied and Computational Mathematics*, **3(3)**: 1879-1895 (2017).

[21] Patel T., Meher R., Thermal Analysis of Porous Fin With Uniform Magnetic Field Using Adomian Decomposition Sumudu Transform Method, Nonlinear Engineering, **6(3)**: 191-200 (2017).

[22] Patel T., Meher R., A Study on Convective-Radial Fins with Temperature-dependent Thermal Conductivity and Internal Heat Generation, *Nonlinear Engineering*, **8(1)**: 145-156 (2019).

[23] Hatami M., Ganji D.D., Thermal Behavior of Longitudinal Convective–Radiative Porous Fins with Different Section Shapes and Ceramic Materials (SiC and Si3N4), *Ceram. Int.*, **40(5)**: 6765-6775, (2014).

[24] Hatami M., Ganji D.D., Thermal And Flow Analysis of Microchannel Heat Sink (MCHS) Cooled by Cu–Water Nanofluid Using Porous Media Approach and Least Square Method, *Energy Conversion and Management*, **78**: 347-358, (2014).

[25] Gorla R.S.R., Bakier A.Y., Thermal Analysis of Natural Convection and Radiation in Porous Fins, *International Communications in Heat and Mass Transfer*, **38(5)**: 638-645, (2011).

[26] Xu R., Weng A., The Calculation for Characteristic Multiplier of Hill's Equation x″+q(t)x=0 in Case q(t) with Positive Mean, *Nonlinear Analysis: Real World Applications*, **9(3)**: 949-962, (2008).

[27] Andrei D. Polyanin , Valentin F. Zaitsev, "Handbook of Exact Solutions for Ordinary Differential Equations", London: CRC Press, Vol. 1. (2002).

[28] Zlatev Z., Dimov Ivan, Faragó, István Havasi, Ágnes, "Richardson Extrapolation: Practical Aspects and Applications", De Gruyter Series in Applied and Numerical Mathematics 2, (2018).

[29] Richardson L.F., The Approximate Arithmetical Solution by Finite Differences of Physical Problems Involving Differential Equations, with an Application to the Stresses in a Masonry Dam, *Philosophical Transactions of the Royal Society of London. Series A, Containing Papers of a Mathematical or Physical Character*, **210**: 307-357 (1911).

[30] Richardson L.F., Gaunt J.A., The Deferred Approach to the Limit. Part I. Single Lattice. Part II. Interpenetrating Lattices, *Philosophical Transactions of the Royal Society of London. Series A, Containing Papers of a Mathematical or Physical Character*, **226**: 299-361 (1927).

[31] Uri M. Ascher, L.R. Petzold, Computer Methods for Ordinary Differential Equations and Differential-Algebraic Equations, *Philadelphia: Society for Industrial and Applied Mathematics*, **332**: (1998).

[32] Polyanin A.D., Zaitsev V.F., "Handbook of Ordinary Differential Equations: Exact Solutions, Methods, and Problems", CRC Press, (2017).